33rd Annual International Conference of the IEEE EMBS
Boston, Massachusetts USA, August 30 - September 3, 2011

Analysis of Cell Cycle Dynamics using Probabilistic Cell Cycle Models

Evren Gurkan-Cavusoglu, *Member, IEEE*, Jane E. Schupp, Timothy J. Kinsella,
Kenneth A. Loparo, *Fellow, IEEE*

***Abstract*— In this study, we develop asynchronous probabilistic cell cycle models to quantitatively assess the effect of ionizing radiation on a human colon cancer cell line. We use both synchronous and asynchronous cell populations and follow treated cells for up to 2 cell cycle times. The model outputs quantify the changes in cell cycle dynamics following ionizing radiation treatment, principally in the duration of both G_1 and G_2/M phases.**

I. Introduction

THE study of the cell cycle kinetics using mathematical models provides a quantitative framework to help identify and develop effective drug targets and multiple drug targeting strategies [1]. The cell cycle kinetics have been modeled using both top-down and bottom-up approaches. The mechanistic models that are based on biochemical modeling of protein dynamics involved in the cell cycle form the bottom-up approaches. The cell cycle kinetics are modeled using ordinary differential equation models in these bottom-up approaches [2-4]. The top-down approaches use a probabilistic approach to model the overall cell cycle kinetics in terms of calculating the distribution of cells among different cell cycle phases [5-9]. Both deterministic and probabilistic cell cycle models are used to study the effects of different treatments on the cell cycle kinetics in [2, 5, 6, 8].

In this work we develop an asynchronous probabilistic cell cycle model to quantitatively analyze cell cycle kinetics of asynchronous cell populations. The model developed here is an extension of our previous model that was developed for synchronous cell populations [10]. The asynchronous model developed here is the most general modeling framework that is capable of capturing cell cycle kinetics of both synchronous and asynchronous cell populations under treatment or no treatment conditions. We have applied the asynchronous cell cycle models to study the effects of ionizing radiation (IR) treatment on the cell cycle kinetics of mismatch repair deficient (MMR-) human colorectal carcinoma cell lines. The DNA mismatch repair system is an important repair mechanism in the cell that ensures genomic stability by correcting mismatches generated during DNA replication and recombination. Mismatch repair deficiencies are known to be associated with certain cancers. The mismatch repair system also contributes to genomic stability by initiating cell death through apoptosis in response to certain DNA damaging agents, so the loss of mismatch repair leads to resistance to chemotherapeutic agents and other types of DNA stress [11], thereby complicating the cancer treatment process.

The chemotherapy resistance of mismatch repair deficient tumors has led to the design of selective treatment strategies toward the treatment of such tumors. One such strategy is to use nucleoside analogs as radiosensitizers in order to increase the sensitivity of deficient cells to ionizing radiation (IR) [12]. We have studied the effect of the radiosensitizer iododeoxyuridine on the cell cycle kinetics of synchronized mismatch repair proficient and deficient cells in [10]. In this work, we have extended the synchronous models such that they apply to asynchronous cell populations, and used these models to study the effect of IR on mismatch repair deficient cells. Our long term goal is to use the models to quantitatively analyze the efficacy of the treatment strategy that combines iododeoxyuridine treatment with IR treatment. The model structure and equations are given in Section II, followed by the modeling results in Section III. Section IV concludes the paper.

This work was supported in part by the NIH grant U56CA112963, NIH grant R21CA140901, the DBJ Foundation, and the University Radiation Medicine Foundation.

E. Gurkan-Cavusoglu is with the Department of Electrical Engineering and Computer Science, Case Western Reserve University, Cleveland, OH 44106 USA, (e-mail: exg44@case.edu).

J. E. Schupp was with Case Western Reserve University, OH 44106 USA. She is now with the Department of Biochemistry, West Virginia University, Morgantown, WV 26506 USA, (e-mail: jschupp@hsc.wvu.edu).

T. J. Kinsella is with the Department of Radiation Oncology, Warren Alpert Medical School of Brown University, Providence, RI 02912, USA, (email: tkinsella@lifespan.org)

K. A. Loparo is with the Department of Electrical Engineering and Computer Science, Case Western Reserve University, Cleveland, OH 44106 USA, (e-mail: kal4@case.edu).

II. Cell Cycle Model

The cell cycle is the cycle of growth and division of cells. It is comprised of four sequential phases; namely gap 1 (G_1), synthesis (S), gap 2 (G_2) and mitosis (M) phases [13]. The gap phases are the phases where the cell growth occurs. The cells duplicate their protein mass and organelles during the gap phases. The suitability of internal and external conditions for S phase and mitosis are also monitored during the G_1 and G_2 phases respectively. The DNA duplication occurs in S phase. M phase is when the chromosome

segregation and cell division occurs. The experimental data we have used in this work is the flow cytometry data that provide the distribution of cells in each cell cycle state for an asynchronous cell population in terms of percentages.

We have modeled the cell cycle using a finite state automaton where the states of the automaton correspond to cell cycle phases. We have first developed these models for synchronous cell populations in [10]. Here, we extend this effort to asynchronous cell populations which is the most general case. The jumps between the states in the finite state automaton model represent transitions from one cell cycle phase to another. The probabilistic jumps are modeled using continuous probability density functions to account for the time spent in each cell cycle phase. The population behavior is obtained by aggregating individual cell models. The probability density function $f_{X\text{-}Y}(t_j|t_i)$ represents the jump from state X to state Y at time t_j, given that the jump to state X occurred at time t_i. The model is shown in Fig. 1, together with an example of the probability density function used in the development of the model. We have used triangular density functions that are defined by two parameters; the mean (m) and the support (v). We have G_2 and M phases lumped together in the model because the experimental data that comes from flow cytometry measurements provide data on the lumped phase instead of the individual G_2 and M phases.

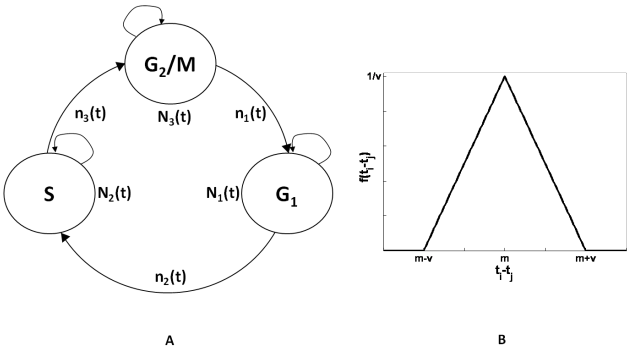

Fig. 1. Probabilistic mathematical model of the cell cycle (panel A) and an example of the probability density function (panel B).

The state variables of the model (n_i's) are the flow of cells into each cell cycle state per unit time. The update equations for each n_i are as follows:

$$\begin{aligned} n_1(t) &= 2\int_{-\infty}^{t} n_3(\lambda) f_3(t-\lambda)d\lambda = 2n_3(t) * f_3(t) \\ n_2(t) &= \int_{-\infty}^{t} n_1(\lambda) f_1(t-\lambda)d\lambda = n_1(t) * f_1(t) \\ n_3(t) &= \int_{-\infty}^{t} n_2(\lambda) f_2(t-\lambda)d\lambda = n_2(t) * f_2(t) \end{aligned} \quad (1)$$

For the equations given in (1), n_1 is the flow into G_1 phase, n_2 is the flow into S phase, and n_3 is the flow into G_2/M phase. The flow into a particular cell cycle phase is calculated as the convolution (denoted by the symbol $*$ on the right hand side of the equations) between the flow into the previous cell cycle phase and the probability density function that represents the jump from this previous cell cycle phase. The equations represent the flow of cells that have left the previous cell cycle phase and have entered the next cell cycle phase. The factor 2 in the equation for n_1 is due to the doubling of the cells leaving the G_2/M phase and entering the G_1 phase.

The total number of cells in each cell cycle phase is calculated as the integral of the difference between the flow of cells into a particular cell cycle phase and the flow of cells leaving that cell cycle phase. The equations for the total cell numbers in each cell cycle phase are given below:

$$\begin{aligned} N_1(t) &= \int_{-\infty}^{t} [n_1(\lambda) - n_2(\lambda)]d\lambda \\ N_2(t) &= \int_{-\infty}^{t} [n_2(\lambda) - n_3(\lambda)]d\lambda \\ N_3(t) &= \int_{-\infty}^{t} [n_3(\lambda) - 0.5n_1(\lambda)]d\lambda \end{aligned} \quad (2)$$

For the equations given in (2), N_1 is the total number of cells in G_1 at time t, N_2 is the total number of cells in S phase, and N_3 is the total number of cells in G_2/M phase. The distributions of cells in each cell cycle phase given as percentages are calculated using the formulas as follows:

$$\begin{aligned} G_1\% &= \frac{N_1}{N_1+N_2+N_3} \times 100\% \\ S\% &= \frac{N_2}{N_1+N_2+N_3} \times 100\% \\ G_2/M\% &= \frac{N_3}{N_1+N_2+N_3} \times 100\% \end{aligned} \quad (3)$$

The initial conditions for the flows n_1, n_2, and n_3 are required to simulate the response of the asynchronous probabilistic cell cycle model given by the Equations 1 – 3. The initial conditions for the treatment cases are calculated from the experimental data for the untreated asynchronous cell populations that are in steady state. The steady state equations for the flows n_1, n_2, and n_3 for the untreated (i.e. no IR) asynchronous cell population are:

$$\begin{aligned} n_1(t) &= x_1 2^{t/t_c} \\ n_2(t) &= x_2 2^{t/t_c} \\ n_3(t) &= x_3 2^{t/t_c} \end{aligned} \quad (4)$$

For the equations given in (4), x_1, x_2, and x_3 are the initial flows at time t=0, and t_c is the cell cycle time for the untreated cell population. The steady state flows are substituted into the equations given in (2), and these equations are then substituted into equations given in (3) to obtain the percentages in each state at steady state as:

$$G_1\% = \frac{N_1}{N_1+N_2+N_3} = \frac{(x_1-x_2)\int_{-\infty}^{t} 2^{\lambda/t_c}\,d\lambda}{0.5x_1\int_{-\infty}^{t} 2^{\lambda/t_c}\,d\lambda} = \frac{x_1-x_2}{0.5x_1} \qquad (5)$$

$$S\% = \frac{N_2}{N_1+N_2+N_3} = \frac{(x_2-x_3)\int_{-\infty}^{t} 2^{\lambda/t_c}\,d\lambda}{0.5x_1\int_{-\infty}^{t} 2^{\lambda/t_c}\,d\lambda} = \frac{x_2-x_3}{0.5x_1}$$

$$G_2/M\% = \frac{N_3}{N_1+N_2+N_3} = \frac{(x_3-0.5x_1)\int_{-\infty}^{t} 2^{\lambda/t_c}\,d\lambda}{0.5x_1\int_{-\infty}^{t} 2^{\lambda/t_c}\,d\lambda} = \frac{x_3-0.5x_1}{0.5x_1}$$

The percentages given in (5) correspond to the steady state percentages measured by flow cytometry for the untreated asynchronous cell populations. The initial flows x_1, x_2, and x_3 can be calculated by comparing the equations given in (5) to the experimental data.

The other parameter that is needed to evaluate steady state equations for the flows n_1, n_2, and n_3 using (4) is the cell cycle time (t_c) for the untreated asynchronous cell population at steady state. This cell cycle time can be calculated from the model parameters for the untreated case. The model development for the untreated case requires that the cells are perturbed from their steady state. This perturbation is obtained by synchronizing the cells by serum starvation for the experimental data presented in this work. The flow cytometry data obtained from the perturbed untreated cell population are then used to estimate the parameters of the model for the untreated asynchronous population. The model equations for the untreated case are the same as the treatment cases, and as given by the equations in (1) – (3). The untreated asynchronous data are used for model initialization, and the initial flows are calculated using the equations given in (4) and (5). The cell cycle time for the untreated cell population model is also estimated during the parameter estimation process.

The model parameters (means and supports) are iteratively estimated using flow cytometry measurements. The cost function used for the model fitting is defined as:

$$\sum_{p=1}^{3}\sum_{t=t_0}^{t_f}\left[d_p(t)-y_p(t)\right]^2 \qquad (6)$$

In equation (6), d_1, d_2 and d_3 are the flow cytometry measurements of the percentages of the cells in G_1, S and G_2/M phases, respectively. The corresponding model outputs for these percentages are represented by y_1, y_2 and y_3, respectively. The inner summation runs for all the experimental time points from the initial time t_0 to the final time t_f. The "fmincon" function of Matlab® (The MathWorks, Inc, Natick, MA) is used for parameter optimization. The parameters are constrained such that the probability density functions have zero value for negative values of time and integrate to one.

III. Results

We have developed asynchronous cell cycle models to quantitatively analyze the cell cycle kinetics of the mismatch repair deficient human colon cancer cell lines. The models are used to analyze the effect of ionizing radiation treatment on cell cycle kinetics of these cancer cells. The experiments were performed on HCT116 cell line. The cells were first synchronized by serum starvation. These untreated cells became less synchronous (asynchronous) within 10 – 12 hrs following release (t=0 hr) into fresh medium. The asynchronous cell populations were then treated with IR (5 Gy) at 13, 16 and 21 hrs following release. IR was delivered using a ^{137}Cs γ-irradiator at 370 cGy/min. Cell cycle profiles for both synchronous untreated cells and IR treated cells were measured using flow cytometry.

The untreated cell populations are synchronized, and the synchronous models we developed previously are adapted for these populations [10]. The IR treatment was applied at later experimental times (t=13, 16 and 21 hrs) when the cells are already asynchronous, so the asynchronous models are used for these cases. The synchronous model equations are essentially the same as the asynchronous model equations just described in (1) – (3) in the manuscript. The primary difference between the synchronous and asynchronous models comes from the definition of the initial flows for n_1, n_2, and n_3. The initial flow derivations for the asynchronous models are discussed above. For the synchronous case, all the cells are assumed to start in G_1 at t = 0 hr, once they are released into complete media. All the other flows are initially assumed to be zero.

The experimental data measures the distributions of the cells for the first and second cell cycles making it possible to estimate the parameters for a second cell cycle. We have two different parameter sets for the first and second cell cycles. Having a second set of parameters for the second and consecutive cell cycles is biologically meaningful since we observed that the cells have a longer first cell cycle time due to recovery from the stress induced by serum starvation, independent of subsequent treatment.

The initial flows for the cell cycle models for IR treatment are obtained from model simulations of the synchronous models developed for the untreated case. The IR is applied at three different time points, i.e. 13, 16 and 21 hrs, and the data from all these three scenarios are combined together for parameter estimation. The results of the model outputs and the model parameters are given in Fig. 2 and Table I respectively. The models successfully captured the dynamics of the cell cycles of the untreated and IR treated cells. The IR treated cells show a G_1 delay in their first cell cycle. IR-treated cells remain in G_1 phase 2 hours longer than the untreated cells. IR-treated cells also show a marked G_2 arrest in their first cell cycle. The parameters for the second cell cycle are not compared due to very low sensitivity values for the IR treated case.

The sensitivity analysis is carried out for each model developed in this work. The parameters of each model are either increased or decreased by 10% one at a time, and the corresponding change in the cost function given in equation (6) is calculated as percent change with respect to the original cost value calculated using the original model

parameters. The parameters that have changed the cost more than 4% on average for a 10% increase or decrease are reported as the parameters that are estimated effectively, and marked as boldface in Table I. The experimental data are sampled every hour, and this affects the sensitivity and estimation of the supports with values less than one hour. The sensitivity analysis is performed by decreasing or increasing the parameters by 10%. This also affects the sensitivity values of the supports due to the fact that changes in the parameters are usually less than an hour, and shorter (< 1 hour) sampling times are required in future experiments to increase the sensitivity to such small changes in the support values.

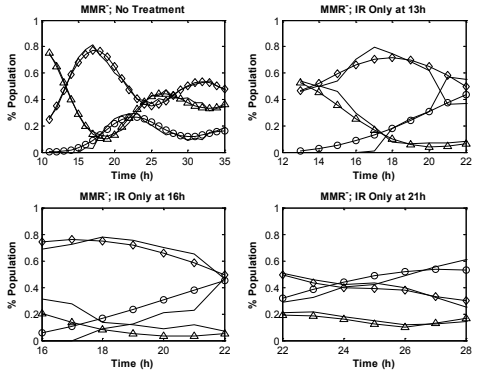

Fig. 2. Asynchronous models for MMR- cells treated with IR. G_1 model (Δ), G_1 experimental data (-); S-phase model (◊), S-phase experimental data (-); and G_2 model (o), G_2 experimental data (-).

TABLE I
MODEL PARAMETERS (m AND v ARE MEASURED IN HOURS)

			MMR-Untreated	MMR-IR
First Cell Cycle	G_1	m_1	**13.19**	**15.23**
		v_1	**7.47**	5.97
	S	m_2	**8.66**	**8.61**
		v_2	**5.53**	8.10
	G_2/M	m_3	**3.47**	**11.06**
		v_3	0.57	11.06
Second Cell Cycle	G_1	m_1	**3.85**	4.65
		v_1	3.85	0.58
	S	m_2	**6.24**	29.92
		v_2	0.74	29.82
	G_2/M	m_3	**2.32**	36.14
		v_3	2.32	26.27

The synchronous model parameters for the untreated cells are effectively estimated. The model for IR treatment is sensitive to first cycle parameters. These models are not very sensitive to the parameters for the second cell cycle parameters. The reason is that IR treatment causes both a G_1 and G_2 arrest in the first cycle, and the first cycle becomes longer. The data are taken for up to 28 hours, and because of the longer first cell cycles, the 28 hours data allow for effective estimation of only the first cell cycle parameters.

IV. Conclusion

The asynchronous cell cycle models developed in this work can be used to quantify the cell cycle kinetics of various cell types under no treatment and treatment conditions. The use of such models allows for the analysis of the effects of different treatments on cell cycle dynamics. These analyses can further be used to guide the design of effective treatment strategies that specifically target the cell cycle kinetics.

References

[1] R. G. Clyde, J. L. Bown, T. R. Hupp *et al.*, "The role of modelling in identifying drug targets for diseases of the cell cycle," *J R Soc Interface,* vol. 3, no. 10, pp. 617-27, Oct 22, 2006.

[2] C. Chassagnole, R. C. Jackson, N. Hussain *et al.*, "Using a mammalian cell cycle simulation to interpret differential kinase inhibition in anti-tumour pharmaceutical development," *Biosystems,* vol. 83, no. 2-3, pp. 91-7, Feb-Mar, 2006.

[3] K. C. Chen, L. Calzone, A. Csikasz-Nagy *et al.*, "Integrative analysis of cell cycle control in budding yeast," *Mol Biol Cell,* vol. 15, no. 8, pp. 3841-62, Aug, 2004.

[4] J. E. Toettcher, A. Loewer, G. J. Ostheimer *et al.*, "Distinct mechanisms act in concert to mediate cell cycle arrest," *Proc Natl Acad Sci U S A,* vol. 106, no. 3, pp. 785-90, Jan 20, 2009.

[5] B. Basse, B. C. Baguley, E. S. Marshall *et al.*, "A mathematical model for analysis of the cell cycle in cell lines derived from human tumors," *J Math Biol,* vol. 47, no. 4, pp. 295-312, Oct, 2003.

[6] P. Hinow, S. E. Wang, C. L. Arteaga *et al.*, "A mathematical model separates quantitatively the cytostatic and cytotoxic effects of a HER2 tyrosine kinase inhibitor," *Theor Biol Med Model,* vol. 4, pp. 14, 2007.

[7] S. S. Pilyugin, V. V. Ganusov, K. Murali-Krishna *et al.*, "The rescaling method for quantifying the turnover of cell populations," *J Theor Biol,* vol. 225, no. 2, pp. 275-83, Nov 21, 2003.

[8] A. Swierniak, A. Polanski, and M. Kimmel, "Optimal control problems arising in cell-cycle-specific cancer chemotherapy," *Cell Prolif,* vol. 29, no. 3, pp. 117-39, Mar, 1996.

[9] P. Ubezio, M. Lupi, D. Branduardi *et al.*, "Quantitative assessment of the complex dynamics of G1, S, and G2-M checkpoint activities," *Cancer Res,* vol. 69, no. 12, pp. 5234-40, Jun 15, 2009.

[10] E. Gurkan, J. E. Schupp, M. A. Aziz *et al.*, "Probabilistic modeling of DNA mismatch repair effects on cell cycle dynamics and iododeoxyuridine-DNA incorporation," *Cancer Res,* vol. 67, no. 22, pp. 10993-1000, Nov 15, 2007.

[11] P. Karran, "Mechanisms of tolerance to DNA damaging therapeutic drugs," *Carcinogenesis,* vol. 22, no. 12, pp. 1931-7, Dec, 2001.

[12] S. E. Berry, and T. J. Kinsella, "Targeting DNA mismatch repair for radiosensitization," *Semin Radiat Oncol,* vol. 11, no. 4, pp. 300-15, Oct, 2001.

[13] B. Alberts, A. Johnson, J. Lewis *et al.*, *Molecular Biology of the Cell* 4th edition ed.: New York: Garland Science 2002.